

Hyperfine Structure of the 6^3P_2 State of $^{80}\text{Hg}^{199}$ and $^{80}\text{Hg}^{201}$. Properties of Metastable States of Mercury*

MARK N. McDERMOTT† and WILLIAM L. LICHTEN‡§
Columbia Radiation Laboratory, Columbia University, New York, New York

(Received January 29, 1960)

The hyperfine structures of the metastable 6^3P_2 state of Hg^{199} and of Hg^{201} have been measured by means of the atomic-beam magnetic resonance technique. The present experiment is the first one for which the electron bombardment method has been used in the production of a narrowly collimated beam of metastable atoms. The beam was detected by surface ejection of electrons from an alkali metal surface. The zero magnetic field intervals $f(F \leftrightarrow F')$ are: for Hg^{199} $f(5/2 \leftrightarrow 3/2) = 22\,666.559(5)$ Mc/sec; and for Hg^{201} $f(7/2 \leftrightarrow 5/2) = 11\,382.6288(8)$ Mc/sec, $f(5/2 \leftrightarrow 3/2) = 8629.5218(5)$ Mc/sec, and $f(3/2 \leftrightarrow 1/2) = 5377.4918(20)$ Mc/sec. The values of the quadrupole and octupole moments of Hg^{201} are, without polarization corrections, $Q = 0.50(4) \times 10^{-24}$ cm² and $\Omega = 0.13$ nuclear magneton barn. The hyperfine structure anomaly for the two isotopes due to the s electron alone is $\Delta(s_{1/2}) = -0.1728(12)\%$ in disagreement with the predictions of the single-particle model.

The g_J values for the 3P_2 state and the $(5d^96s^26p)^3D_3$ state were found to be $g_J(^3P_2) = 1.50099(10)$ and $g_J(^3D_3) = 1.0867(5)$. The value of $J=3$ for the 3D_3 state was confirmed. A new technique for obtaining excitation functions is discussed.

I. INTRODUCTION

THE atomic beam magnetic resonance method has been extended recently to the measurement of the hyperfine structure of the metastable 3P_2 states of the elements of Groups II and VIII of the periodic table.¹⁻⁴ If configuration interaction is neglected the wave function of the 3P_2 state can be expressed simply as $(s_{1/2})(p_{3/2})^{\pm 1}$ in jj coupling. The s electron has a large magnetic dipole interaction while the $p_{3/2}$ electron or hole can interact with the nuclear electric quadrupole and magnetic octupole moments, if they exist, in addition to the magnetic dipole moment. A number of the elements of Groups II and VIII possess two stable isotopes of odd nucleon number A . In such cases one can obtain a hyperfine structure anomaly. Anomalies for odd-neutron, even-proton isotopes such as those in Groups II and VIII have not been measured previously.

Natural mercury has two isotopes which have non-zero spin, Hg^{199} with $I=1/2$ and Hg^{201} with $I=3/2$. Hg^{199} has an abundance of 16.84% and Hg^{201} an abundance of 13.22%.⁵ In zero external magnetic field the 3P_2 state of Hg^{199} is split into two levels with total angular momenta $F=5/2$ and $3/2$. The 3P_2 state of

Hg^{201} is split into four levels characterized by $F=7/2$, $5/2$, $3/2$, and $1/2$. From a measurement of the splittings it is possible to obtain values of the magnetic dipole interaction constants in both isotopes and the quadrupole and octupole interaction constants in Hg^{201} .

A very large number of measurements of the hyperfine structure of the 6^3P_2 state of Hg^{199} and Hg^{201} have been made optically. Recent measurements are collected in Table I, together with our values for comparison. This paper describes a measurement of the hyperfine structure extending the precision of the optical measurements by a factor of 1000.

II. EXPERIMENTAL METHOD

A. General Method

The general experimental arrangement is illustrated schematically in Fig. 1. Mercury atoms in the ground state issue from the slit in a conventional iron oven heated to approximately 125°C. Immediately in front of the oven the atoms are bombarded with electrons of an energy optimum for exciting them into the 3P_2 state.

TABLE I. Optical hyperfine structure measurements.

Investigators	Hg^{199}		Hg^{201}	
	$5/2 \leftrightarrow 3/2$	$7/2 \leftrightarrow 5/2$	$5/2 \leftrightarrow 3/2$	$3/2 \leftrightarrow 1/2$
Görlich and Lau ^a	746 ^a	-(374.6) ⁱ	-287	-180
Schüler and Schmidt ^b	756.6 ^b	-379.7	-288.1	-179.6
Burger and van Cittert ^c	756	-381	-283	-182
Murakawa ^d	759	-380	-287	-179.6
Korolev and Odintsov ^e	757	-379	-287	-179
Blaise and Chantrell ^f	757.3	-379.0	-288.4	-180.0
Present work	756.0750 ⁱ	-379.6829	-287.8493	-179.3735

^a P. Görlich and E. Lau, Z. Physik **77**, 746 (1932).

^b H. Schüler and T. Schmidt, Z. Physik **98**, 239 (1935).

^c H. C. Burger and P. H. van Cittert, Physica **5**, 177 (1938).

^d K. Murakawa, Phys. Rev. **78**, 480 (1950).

^e F. A. Korolev and V. I. Odintsov, Optika i Spektroskopiya **1**, 17 (1956).

^f J. Blaise and H. Chantrell, J. phys. radium **18**, 193 (1957).

^g All intervals are in units of 10^{-9} cm⁻¹.

^h Schüler's value has been corrected for a computational error.

ⁱ $c = 299\,793.0$ km/sec.

^j The $7/2 \leftrightarrow 5/2$ interval has been calculated from the $5/2 \leftrightarrow 3/2$ and $3/2 \leftrightarrow 1/2$ intervals.

* Work supported in part by the Office of Naval Research, and the Signal Corps, and the Air Force Office of Scientific Research under a joint service contract and an Office of Naval Research Contract.

† Submitted in partial fulfillment of the requirements for the degree of Doctor of Philosophy in the Faculty of Pure Science, Columbia University.

‡ Present address: Ryerson Physical Laboratory, University of Chicago, Chicago 37, Illinois.

§ National Science Foundation postdoctoral fellow 1956-1957.

¹ W. Lichten and M. McDermott, Bull. Am. Phys. Soc. **3**, 186 (1958).

² W. Faust, M. McDermott, and W. Lichten, Bull. Am. Phys. Soc. **3**, 371 (1958).

³ G. M. Grosf, P. Buck, W. Lichten, and I. I. Rabi, Phys. Rev. Letters **1**, 214 (1958).

⁴ A. Lurio, Bull. Am. Phys. Soc. **4**, 419 and 429 (1959).

⁵ A. O. Nier, Phys. Rev. **79**, 450 (1950).

The resulting metastable atoms then pass through a conventional magnetic resonance apparatus and in the absence of a transition are focused on a stop wire. If a transition occurs they miss the stop and strike an alkali metal surface from which they eject electrons. The electron current is then amplified in a standard electrometer circuit and the signal is ultimately observed as a galvanometer deflection.

B. Production of Metastables

The original source of metastables was a water-cooled, low-pressure mercury arc. This source resulted in a large unavoidable photon background, and at best the estimated signal to noise ratio of a transition between single hyperfine levels was 2/1.

The electron bombardment source finally adopted has decided advantages for use with collimated beams. Collimation before bombardment greatly increases the ratio of the effective solid angle for the metastables to the effective solid angle for photons at the detector over the same ratio for a discharge source.⁶ Another important advantage is that the electron energy can be controlled within narrow limits. It might be expected that

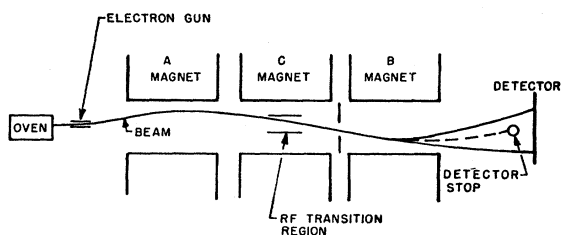


FIG. 1. Schematic of apparatus.

the effects of recoil would destroy the collimation thus making such a method unsuitable for cases where very close beam definition is necessary. However, if the electron gun is placed very close to the source slit the loss of intensity by scattering out of the beam is not great since it is at least in part compensated by a scattering of particles into the beam.

The electron gun is shown schematically in Fig. 2. A tungsten filament was stretched a few thousandths of a centimeter below a U-shaped copper collector. A magnetic field of approximately 700 gauss collimated the electron beam. The atomic beam entering from the end of the collector was bombarded by the electrons in the roughly equipotential region within the collector. The signal to noise ratio for a single transition in Hg^{201} was usually 20/1 or better with the bombardment source.

The 3P_2 state has a lifetime of approximately 0.1 second if the principal mode of decay is assumed to be a magnetic dipole transition to the 3P_1 state. With a typical beam velocity of 2×10^4 cm/sec there is essen-

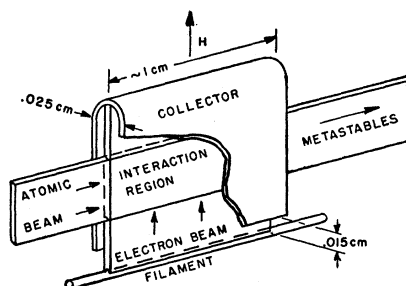


FIG. 2. Schematic of electron gun.

tially no decay from this state within the 30-cm apparatus length.

C. Deflecting Fields

Chiefly because of mechanical limitations the deflecting magnets were operated at intermediate field for the Zeeman effect of the hyperfine structure. To determine which transitions were observable and the relative intensities of the transitions, the magnetic moments of the states were obtained as a function of magnetic field. From an expression for the energy W as a function of magnetic field H the magnetic moment $\mu = -\partial W / \partial H$ was obtained. For Hg^{199} the energies of the various magnetic substates were computed exactly by a slight variation of the Breit-Rabi formula.⁷ The

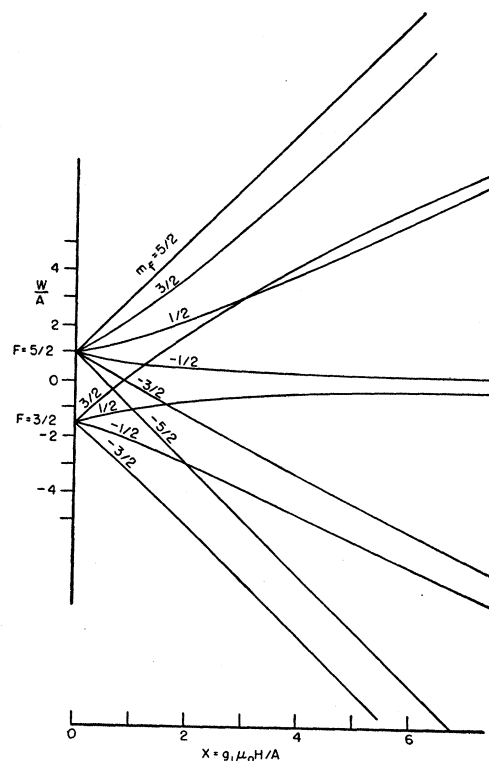


FIG. 3. Zeeman effect of the hyperfine structure of Hg^{199} .

⁶ W. Lichten, J. Chem. Phys. 26, 306 (1956).

⁷ G. Breit and I. I. Rabi, Phys. Rev. 38, 2082 (1931).

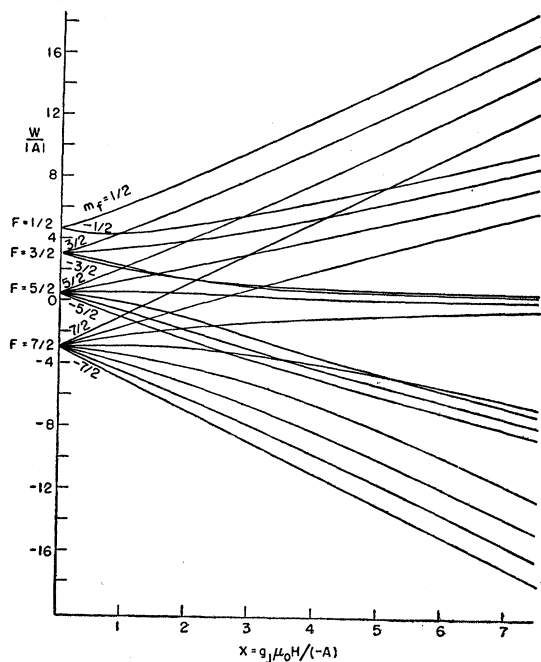


FIG. 4. Zeeman effect of the hyperfine structure of Hg^{201} .

energies are shown in Fig. 3. For the 3P_2 state of Hg^{201} , in which $I=3/2$ and $J=2$, an IBM-650 computer was used to extract the eigenvalues of the energy matrix. The quadrupole interaction was included in the Hamiltonian but the small octupole interaction was omitted. The resultant Hamiltonian is

$$\frac{W}{|A|} = -h\mathbf{I} \cdot \mathbf{J} - \frac{B}{A} \left(\frac{\mathbf{I} \cdot \mathbf{J}(2\mathbf{I} \cdot \mathbf{J} + 1) - I(I+1) - J(J+1)}{2I(2I-1)(J)(2J-1)} \right) + \left(J_z + \frac{g_I}{g_J} I_z \right) x,$$

where $x = (g_J \mu_0 H)/(-A)$ and H is the magnetic field assumed to be in the z direction. The constants were taken to be $B/A = -0.119128$ and $g_I/g_J = +1.340 \times 10^{-4}$. Eigenvalues were obtained for 40 values of the magnetic field. The resultant energy levels are plotted in Fig. 4. The deflecting fields ranged from 1500 to 3000 gauss corresponding to a range in x , for Hg^{201} , of $x=1$ to $x=2$ and, for Hg^{199} , of $x=0.4$ to $x=0.8$.

D. Detection

Two methods of detecting mercury metastables have been reported. The first depends on the fact that it is energetically possible for a metastable atom impinging on a hot tungsten surface to be evaporated as an ion. This process can occur if the energy required to ionize the metastable, 4.87 volts for mercury, is less than the work function of the tungsten surface. An oxygenated tungsten surface can have a work function considerably exceeding 4.87 volts so that surface ionization would

appear possible and has been reported by Bühl.⁸ This scheme was tried without success in some preliminary experiments.⁹ Hagstrum,¹⁰ on the other hand, argues that, for a clean surface, ions so formed would be immediately neutralized by an Auger process. It is not clear what happens for an oxidized surface, but due to some process such as Hagstrum mentions it may, indeed, not be possible to obtain mercury ions in this manner.

The second method is based on the observation¹¹ that a mercury metastable striking certain metal surfaces will eject an electron. Surface ejection of an electron has been discussed in detail by Hagstrum¹² as a possible consequence of Auger de-excitation of the metastable or of resonance ionization followed by Auger neutralization. It can occur provided the excitation energy of the metastable state is greater than the work function of the surface. According to Hagstrum's discussion the electron ejection efficiency is dependent on, among other things, the number of electrons which have energies $\epsilon \geq \epsilon_0 - E_x$, where ϵ and ϵ_0 are, respectively, the energy of the electron and the energy of the vacuum level measured above the bottom of the conduction band and E_x is the excitation energy of the metastable. The alkali metals, which have low work functions and narrow conduction bands, are especially suitable detectors for mercury as all electrons in the conduction band satisfy $\epsilon \geq \epsilon_0 - E_x$ except in lithium.¹³ However, it is apparent that all the electrons need not have energies which satisfy this condition for detection to occur.

Sodium evaporated under vacuum within the apparatus was used as a detector in nearly all the measurements. A good surface once obtained usually suffered little or no deterioration during a run of five or six hours. In the last measurements rubidium was also used. This surface has a somewhat higher detection efficiency.

E. rf Apparatus

The general arrangement used in the hyperfine structure measurements for generating and measuring the rf signal is illustrated in Fig. 5 and is similar to that used by Ting and Lew.¹⁴ Three different klystrons were used to cover the required frequency range: a Raytheon 2K33A at 22 700 Mc/sec, a Varian X-13 at 11 400 Mc/sec and 8600 Mc/sec, and a Varian VA221H at 5400 Mc/sec.

A cavity wavemeter was used to make a frequency measurement to within 3–6 Mc/sec. For precision measurement the klystron signal was beat against a multiple of the output of a crystal controlled frequency

⁸ A. Bühl, *Helv. Phys. Acta* **6**, 231 (1933).

⁹ Performed by P. Kusch and one of us, W.L.L.

¹⁰ H. D. Hagstrum (private communication, to be published).

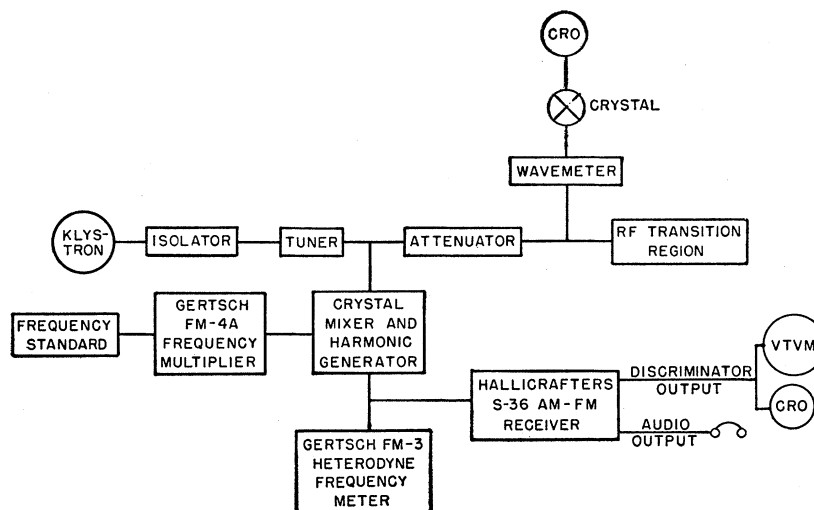
¹¹ H. Webb, *Phys. Rev.* **24**, 113 (1924).

¹² H. D. Hagstrum, *Phys. Rev.* **96**, 336 (1954).

¹³ W. Lichten, *Phys. Rev.* **109**, 1191 (1958).

¹⁴ Y. Ting and H. Lew, *Phys. Rev.* **105**, 581 (1957).

FIG. 5. Block diagram of rf generating and measuring equipment.



standard. The frequency of the beat note was measured either by obtaining an audio zero beat between the beat note and a signal from a Gertsch FM-3 heterodyne frequency meter, or by introducing the beat note into an FM receiver previously calibrated against the FM-3 and measuring the dc voltage output of the receiver discriminator.

Except for a few preliminary measurements, the rf transition region was a shorted waveguide tapered to fit between the pole faces of the C magnet and slotted to permit passage of the beam. Waveguide sizes were chosen so that only the lowest, TE_{10} , mode was propagated and thus the rf magnetic field was everywhere perpendicular to the static field. This polarization meant that only the π transitions, $\Delta m_F = \pm 1$, could be seen. For all except the lowest frequency transition in Hg^{201} a second hairpin was placed immediately beside the waveguide hairpin. The hairpin was a conventional, shorted, parallel conductor type and could be used to excite transitions at low frequencies, i.e., the transitions $\Delta m_F = \pm 1$, $\Delta F = 0$. Three hairpins of different lengths along the beam were used for the frequency range covered: one at 22 700 Mc/sec, a second at 11 400 Mc/sec and 8600 Mc/sec and a third at 5400 Mc/sec.

III. METASTABLE STATES OF MERCURY

A. 3D_3 State

In one of the important investigations of the term structure of mercury Murakawa¹⁵ first observed the $(5d^96s^26p)^3D_3$ state in combination with higher lying states of the configuration $6snd$. At that time it was not understood why this state was not observed to decay to lower lying states. In preliminary work¹³ a metastable state was found which was identified with the 3D_3 state on the basis of energy. The lifetime of the state was measured to be greater than 10^{-2} second which

¹⁵ K. Murakawa, Z. Physik **108**, 168 (1938).

explains the failure to observe the combination of the state with lower lying states. Since that time Murakawa¹⁶ has calculated a wave function for the 3D_3 state using the method of Hume and Crawford¹⁷ and has obtained $\Psi(^3D_3) = K_1\psi[^3D_3(d^9p)] + K_2\psi[^3F_3(d^9p)] + K_3\psi[^1F_3(d^9p)] + K_4\psi[^3F_3(sf)] + K_5\psi[^1F_3(sf)]$, where $K_1 = 0.3251$, $K_2 = 0.7329$, $K_3 = -0.5955$, $K_4 = -0.0384$, $K_5 = 0.0312$. As a result of the presence of $^3F_3(sf)$ and $^1F_3(sf)$ character in the wave function, atoms in the 3D_3 state can make allowed electric dipole transitions to the lower lying $(6s6d)^3D_{3,2}$ and $(6s6d)^1D_2$ states. With Murakawa's values for K_4 and K_5 the lifetime is computed as $\tau \approx 6 \times 10^{-2}$ second in agreement with the observed lifetime. Murakawa has used the wave function to compute $g_J(^3D_3) = \sum_i K_i^2 g_J(\psi_i) = 1.08$ with an uncertainty which is stated to be 4%.

B. Excitation Functions

An excitation function taken for mercury in the normal manner shows two superposed peaks¹³ corresponding to two metastable states, the 6^3P_2 state and the 3D_3 state. The combination of an electron bombardment source and a Rabi magnetic resonance apparatus has made it possible to obtain separate excitation functions for the two states since atoms in the two states have quite different magnetic moments. To achieve the separation the oscillator was set at a frequency which gave a maximum intensity in the transitions $\Delta J = 0$, $\Delta m_J = \pm 1$, $\nu = g_J \mu_0 H / h$ in the even A isotopes. As the electron energy was increased the signal from those atoms undergoing a transition was obtained as the difference between the signal with rf on and rf off. In general, as long as two states, 1 and 2, have g_J values which differ sufficiently so that $[g_J(1) - g_J(2)] \mu_0 H / h$

¹⁶ K. Murakawa, J. Phys. Soc. Japan **14**, 1624 (1959), and private communications.

¹⁷ J. N. P. Hume and M. F. Crawford, Phys. Rev. **84**, 486 (1951).

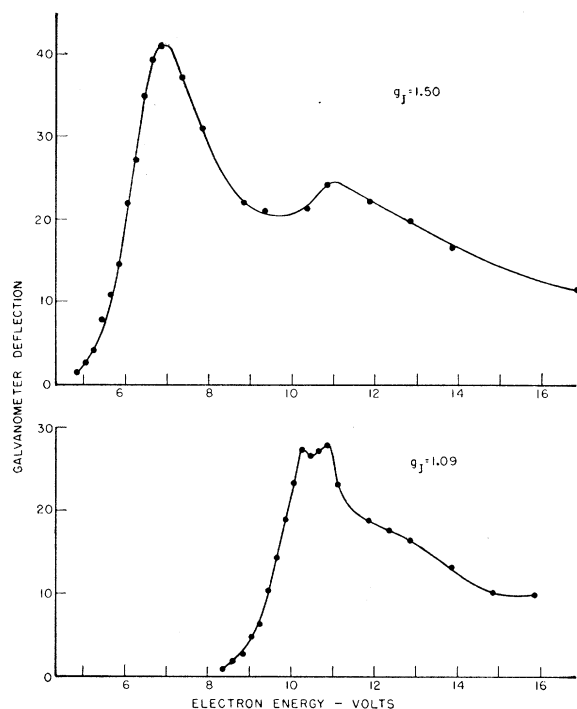


FIG. 6. Excitation functions for the 3P_2 ($g_J=1.50$) and 3D_3 ($g_J=1.09$) states of mercury.

is appreciably greater than the width of a single resonance, the procedure will give separate excitation functions.

Two excitation functions obtained as described are shown in Fig. 6. The electron energy scale has been adjusted so that the appearance potential for the 3P_2 state ($g_J=1.50$) is 5.4 volts. The potential was verified previously against the known appearance potential of $\text{He}({}^3S_1)$.⁶ The appearance potential for the 3D_3 state ($g_J=1.09$) was 9.0 volts in good agreement with the spectroscopic value¹⁵ of 9.05 volts. An investigation at an electron energy of 7.0 volts showed no rf induced signal at a frequency corresponding to $g_J=1.09$ and thus confirmed that the resonances for the 3P_2 and 3D_3 states were well separated. The data do not exclude the possibility of the excitation of other metastable states with $g_J \approx 1.50$. As the apparatus was not suited for measuring cross sections the excitation functions should not be relied on for more than a qualitative indication of the dependence of the excitation cross section on electron energy. Also, the magnitude of the signals should not be interpreted as a measure of the relative cross sections for the excitation of the two states.

C. g_J Values

The g_J values for the 3P_2 and 3D_3 states were measured and further confirmed the identification of the latter. The general arrangement was similar to that described for the hyperfine structure measurements with the addition of a gas line which led from an argon supply

through a controlled gas leak into the mercury oven. With the leak closed and the electron energy at about 7 volts a beam of metastable mercury in the 3P_2 state was obtained, while at 10.5 volts atoms in both the 3P_2 and 3D_3 states were present. If the leak was opened and the energy raised to about 18 volts the beam consisted of both mercury and argon metastables. In order to detect argon and not mercury 3P_2 metastables the alkali detector was removed and a tungsten stop wire, which does not detect mercury 3P_2 metastables appreciably but does detect argon, was used as a detector. For argon the signal corresponded to a decrease in the number of atoms striking the stop wire while for mercury 3P_2 and 3D_3 metastables the signal corresponded to an increase in the number of atoms striking the alkali detector. The magnetic field in the transition region was set at approximately 25 gauss. Resonances corresponding to the Zeeman transitions $\Delta m_J = \pm 1$ were observed successively in the 3P_2 states of both argon and the even isotopes of mercury. Resonances in the 3D_3 state were measured alternately with resonances in the mercury 3P_2 state. Since the resonance frequencies are just $\nu = g_J \mu_0 H / h$, the ratios of the frequencies are directly the ratios of the g_J values.

For the measurement of the ratio $g_J({}^3P_2, \text{Hg}) / g_J({}^3P_2, \text{A})$ two mercury and four argon resonance curves were obtained. In the determination of $g_J({}^3D_3, \text{Hg}) / g_J({}^3P_2, \text{Hg})$ two 3D_3 resonances and four mercury 3P_2 resonances were obtained. The measurements give

$$g_J({}^3P_2) = 1.50099(10),$$

$$g_J({}^3D_3) = 1.0867(5),$$

where the value for $g_J({}^3P_2)$ for argon is taken to be $g_J = 1.500964(8)$.¹⁸ The experimental uncertainties in the last digits are given in parentheses. The attainable experimental accuracy was limited chiefly by magnetic field inhomogeneities.

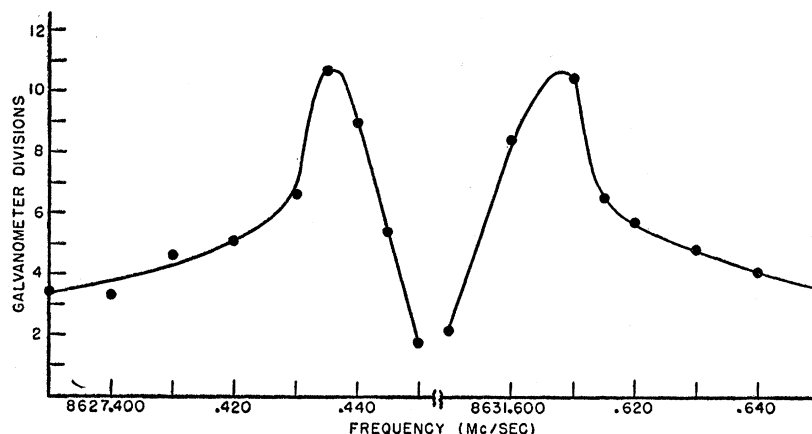
The value for $g_J({}^3P_2)$ which is calculated with the vector model for $g_l=1$ and $g_s=2(1.00116)$ is $g_J = 1.50116$. A number of small corrections discussed by Abragam and Van Vleck¹⁹ have not been evaluated. The measured $g_J({}^3D_3)$ is in satisfactory agreement with the value calculated by Murakawa. An additional confirmation of the identification of the higher lying metastable state was obtained by observing the number and spacing of the low field $\Delta F=0$, $\Delta m_F = \pm 1$ transitions in the odd A isotopes. For a given value of J and for $I=1/2$ there are two values of g_F , and for $J \geq 3/2$, $I=3/2$ there are four values. The ratios of the frequencies of the low field transitions are just the ratios of the g_F values and are different for each value of J .

Although the signal was adequate for a measurement of the hyperfine splitting in the 3D_3 state such a measurement was not undertaken. The electronic structure

¹⁸ A. Lurio, C. Drake, V. W. Hughes, and J. A. White, Bull. Am. Phys. Soc. **3**, 8 (1958).

¹⁹ A. Abragam and J. H. Van Vleck, Phys. Rev. **92**, 1448 (1953).

FIG. 7. Symmetric pair, $(5/2, 1/2) \leftrightarrow (3/2, -1/2)$, $(5/2, -1/2) \leftrightarrow (3/2, 1/2)$, observed for Hg^{201} .



of the state is not well enough understood at present so that any useful information about nuclear properties could be obtained beyond that available from a measurement in the 3P_2 state.

IV. HYPERFINE STRUCTURE MEASUREMENTS

A. General Method

To determine the frequency of a resonance the klystron was set at a series of closely spaced frequencies and the difference between the metastable signal with rf on and rf off was noted. Usually a fairly complete resonance was observed. The resonance frequency was graphically obtained from a curve plotted through the observed points.

In preliminary measurements on a particular hyperfine structure interval a search was made for all transitions of the type $\Delta F = \pm 1$, $\Delta m_F = 0, \pm 1$ which the rf polarization would allow. In each case a sufficient number of transitions was observed so that they could be unambiguously identified from their spacings.

The final observations were made on lines whose magnetic field dependence was equal and opposite. Although the π transitions have the advantage of involving relatively large moment changes at intermediate fields, they suffer from the disadvantage of having a large magnetic field dependence at low fields. As a result small field inhomogeneities could distort and broaden the resonances and such broadening was observed in nearly all the lines measured. It is reasonable to expect, however, that for lines with frequencies of equal and opposite field dependence the distortion will also be equal and opposite. One such symmetric pair is illustrated in Fig. 7. The field in this case produced much more distorted lines than those used in the final measurements but the lines do illustrate the anticipated symmetry about the zero field interval. The average of the frequencies of some similar feature of these lines should then be the zero field hyperfine interval except for a small correction quadratic in the magnetic field.

B. Details of Measurements

Hg^{199} $F=5/2 \leftrightarrow F=3/2$. The spectrum observed is shown in Fig. 8. Six π transitions of the eight possible ones were observed. Of these, the symmetric pair $(5/2, -1/2) \leftrightarrow (3/2, 1/2)$, $(5/2, 1/2) \leftrightarrow (3/2, -1/2)$ was used for all final measurements. If a run is defined as a set of measurements for which all significant experimental parameters were unchanged, three runs were taken involving the observation of a total of twelve symmetric pairs. The results are shown in Table II.

The value of the zero-field splitting is the average of the frequencies of the two transitions comprising the symmetric pair except for the quadratic correction. This correction was 300 cps for the highest field used and has been made in the final results given in Table II. The linewidths varied between the runs from a natural linewidth of 50 kc/sec to a broadened line of 105 kc/sec width for one set of data.

Hg^{201} $F=7/2 \leftrightarrow F=5/2$. Seven of the twelve possible π transitions were seen and are shown in Fig. 9. The

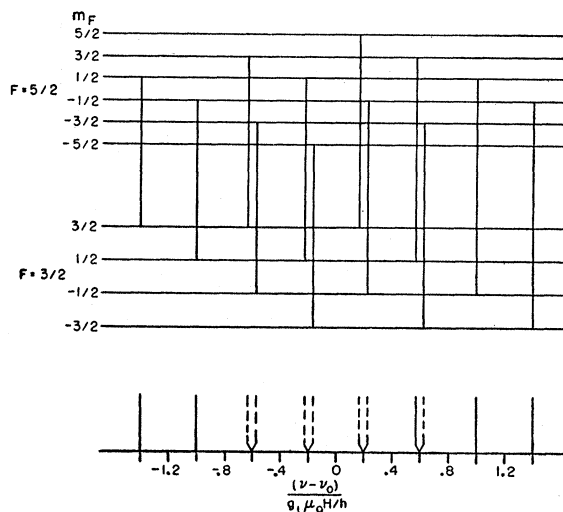


FIG. 8. Spectrum for $F=5/2 \leftrightarrow F=3/2$ transitions in Hg^{199} . ν_0 is the zero-field hyperfine structure splitting. Observed transitions are indicated by solid lines.

TABLE II. Zero field hyperfine structure intervals for individual runs.

	Interval	Frequency	Standard deviation of mean	Number of symmetric pairs
Hg ¹⁹⁹	$F=5/2 \leftrightarrow F=3/2$	22 666.5628	(19)	2
		22 666.5619	(20)	4
		22 666.5559	(9)	6
	Average	22 666.5591	(12)	
Hg ²⁰¹	$F=5/2 \leftrightarrow F=7/2$	11 382.62877	(26)	4
		11 382.62809	(46)	3
		11 382.62870	(14)	4
		11 382.62945	(27)	3
	Average	11 382.62875	(18)	
Hg ²⁰¹	$F=3/2 \leftrightarrow F=5/2$	8629.52170	(10)	3
		8629.52150	(20)	3
		8629.52202	(33)	3
		8629.52196	(30)	3
	Average	8629.52180	(10)	
Hg ²⁰¹	$F=1/2 \leftrightarrow F=3/2$	5377.49077	(11)	3
		5377.49340	(11)	3
		5377.49195	(10)	3
		5377.49109	(35)	3
	Average	5377.49180	(32)	

definitive determinations were made with the use of the symmetric pair $(7/2, -1/2) \leftrightarrow (5/2, 1/2)$, $(7/2, 1/2) \leftrightarrow (5/2, -1/2)$. The line widths were approximately 12 kc/sec. The quadratic correction was in no case larger than 80 cps.

Hg²⁰¹ $F=5/2 \leftrightarrow F=3/2$. Five of the possible eight π transitions were observed as shown in Fig. 10. Four runs of three pairs each were taken on the symmetric pair $(5/2, 1/2) \leftrightarrow (3/2, -1/2)$, $(5/2, -1/2) \leftrightarrow (3/2, 1/2)$. The line widths were of the order of 14 kc/sec and indicate some broadening due to field inhomogeneities. The largest quadratic correction amounted to 300 cps.

Hg²⁰¹ $F=3/2 \leftrightarrow F=1/2$. Preliminary data on this line were taken with a hairpin which permitted σ as well as π transitions to be seen. Consequently, as is shown in Fig. 11, the two possible σ transitions were observed. The $F=3/2 \leftrightarrow F=1/2$ hyperfine interval was

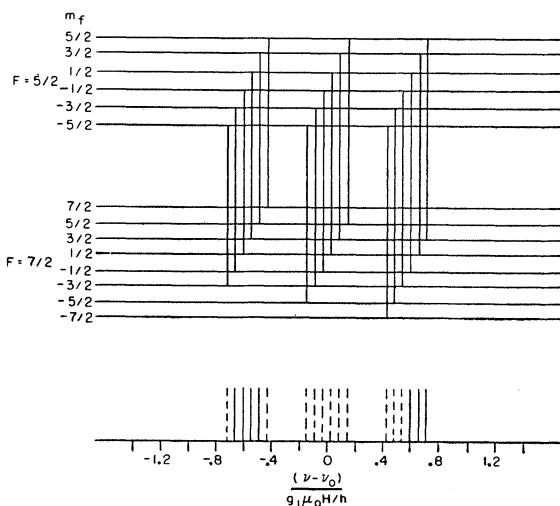


FIG. 9. Spectrum for $F=5/2 \leftrightarrow F=7/2$ transitions in Hg²⁰¹. ν_0 is the zero-field hyperfine structure splitting. Observed transitions are indicated by solid lines.

the only one for which symmetric pairs were not observed. The lines used were $(3/2, -1/2) \leftrightarrow (1/2, 1/2)$, which has a linear field dependence of $+1.4 (g_J \mu_0 H)/h$ at low fields, and $(3/2, -3/2) \leftrightarrow (1/2, -1/2)$ which has a dependence of $+0.2 (g_J \mu_0 H)/h$. The much lower field dependence of the second transition resulted in a narrow but somewhat distorted line of about 8 kc/sec width. The more field-dependent line was as wide as 30 kc/sec and quite distorted. However, a given uncertainty in the frequency of this line contributes a relatively smaller amount to the uncertainty of the hyperfine interval than does an equal uncertainty in the less field-dependent line.

V. DISCUSSION OF ERRORS

The data were taken in such a way as to compensate for several possible systematic errors. The hairpin was rotated 180° in one-half of the data to compensate for

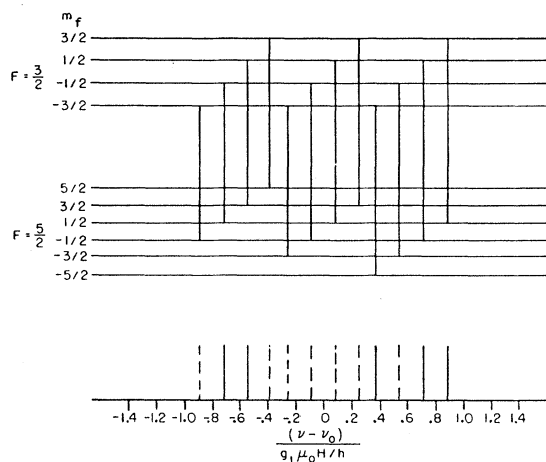


FIG. 10. Spectrum for $F=3/2 \leftrightarrow F=5/2$ transitions in Hg²⁰¹. ν_0 is the zero-field hyperfine structure splitting. Observed transitions are indicated by solid lines.

the effect on the zero-field interval of a possible rf phase shift along the beam direction. Equal numbers of determinations were made with the two possible static field directions; thus no net error arising from the Millman effect²⁰ should occur in the average of the data. A possible shift in the resonance which might arise from changing rf amplitude along the beam direction cannot be discounted. Effects associated with the rf power are believed to contribute insignificantly to the error. The Bloch-Siegert effect²¹ is insignificant for the large hyperfine separations measured. The uncertainty in the frequency measurement due to fluctuations in the frequency standard was estimated to be 3 parts in 10⁸.

To allow for possible systematic effects associated with the inhomogeneous field as well as a possible unfavorable accumulation of errors in the fairly small

²⁰ S. Millman, Phys. Rev. **55**, 628 (1938).

²¹ F. Bloch and A. Siegert, Phys. Rev. **57**, 522 (1940).

body of data taken, limits of error have been arbitrarily taken as three times the standard deviation of the mean of all runs on a given hyperfine interval. In arriving at the standard deviation each pair was treated as a single observation.

VI. RESULTS AND DISCUSSION

The final experimental values for the zero-field intervals are

$$\begin{aligned} \text{Hg}^{199} f(5/2 \leftrightarrow 3/2) &= 22\ 666.559(5) \text{ Mc/sec;} \\ \text{Hg}^{201} f(7/2 \leftrightarrow 5/2) &= 11\ 382.6288(8) \text{ Mc/sec,} \\ f(5/2 \leftrightarrow 3/2) &= 8629.5218(5) \text{ Mc/sec,} \\ f(3/2 \leftrightarrow 1/2) &= 5377.4918(20) \text{ Mc/sec.} \end{aligned}$$

Although first order perturbation theory is generally adequate for obtaining the magnetic dipole and electric quadrupole interaction constants, earlier work²² has

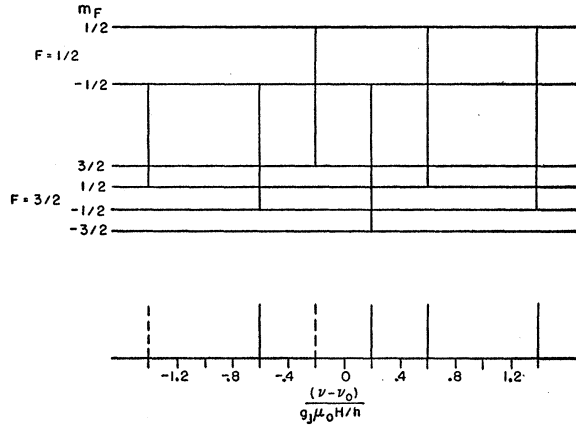


FIG. 11. Spectrum for $F=1/2 \leftrightarrow F=3/2$ transitions in Hg^{201} . ν_0 is the zero-field hyperfine structure splitting. Observed transitions are indicated by solid lines.

shown that in all cases thus far investigated a second order treatment results in sizable corrections to the magnetic octupole interaction as derived from first order theory. In the case of Group III and Group VII elements of the periodic table which have a single p valence electron or hole the second order perturbation can be adequately approximated by considering the neighboring doublet level only. Similarly, for the $n\ ^3P_2$ state of an $nsnp$ configuration a first approximation is to consider perturbations by the $n\ ^3P_{1,0}$ and $n\ ^1P_1$ states only.

The theory of the hyperfine structure of the perturbing states has been carried out in intermediate coupling by Breit and Wills.²³ The wave functions for the 3P_2 and 3P_0 states are the same in either jj or LS coupling while the wave functions for the $^1,^3P_1$ states are ex-

pressed in intermediate coupling as the sums of products of jj coupling wave functions for the individual electrons.

$$\begin{aligned} \psi(^3P_1) &= c_1(1/2, 3/2) + c_2(1/2, 1/2), \\ \psi(^1P_1) &= c_1'(1/2, 3/2) + c_2'(1/2, 1/2), \end{aligned}$$

where $c_1' = c_2$ and $c_2' = -c_1$. To carry the theory of the hyperfine structure of the 3P_2 state to second order it is necessary to obtain matrix elements of the general hyperfine structure interaction between this state and all other states for which the matrix elements do not vanish. The magnetic dipole interaction connects states which differ in J by no more than ± 1 ; the electric quadrupole interaction connects states which differ in J by no more than ± 2 . The effect of higher order multipole interactions is completely negligible. Thus for an approximation which considers perturbations by other states of the configuration only, it is necessary to have the matrix elements of the dipole and quadrupole operators between the 3P_2 state and the 3P_1 and 1P_1 states and of the quadrupole operator alone between 3P_2 and 3P_0 states. These matrix elements have been evaluated and in the notation of Schwartz²² are, for the magnetic dipole interaction,

$$\begin{aligned} \langle ^3P_2 IF | \sum_a T_q^{(1)}(e) T_{-q}^{(1)}(n) (-1)^q | ^3P_1 IF \rangle \\ = -\frac{1}{4} [(F+I+3)(F-I+2)(I-F+2)(F+I-1)]^{1/2} \\ \times [c_1 a_s / 2 - (\frac{1}{2} c_1 + \frac{5}{16} \sqrt{2} c_2 \xi) a_{3/2}], \end{aligned}$$

where a_s is the dipole interaction constant for the s electron and $a_{3/2}$ the same quantity for the $p_{3/2}$ electron. $T_q^{(k)}(e)$ and $T_q^{(k)}(n)$ are tensor operators of rank (k) operating on the electron coordinates only and the nuclear coordinates only, respectively. The corresponding matrix element between the 3P_2 and 1P_1 states is obtained by replacing c_1 and c_2 by c_1' and c_2' . The off-diagonal quadrupole matrix elements are

$$\begin{aligned} \langle ^3P_2 IF | \sum_a T_q^{(2)}(e) T_{-q}^{(2)}(n) (-1)^q | ^3P_1 IF \rangle \\ = -\frac{1}{16I(2I-1)} [(F+I+3)(F-I+2) \\ \times (I-F+2)(F+I-1)]^{1/2} \\ \times [I(I+1) - F(F+1) + 3] [c_1 + \sqrt{2} c_2 \eta] b_{3/2}, \end{aligned}$$

where $b_{3/2}$ is the quadrupole interaction constant for the $p_{3/2}$ electron, and

$$\begin{aligned} \langle ^3P_2 IF | \sum_a T_q^{(2)}(e) T_{-q}^{(2)}(n) (-1)^q | ^3P_0 IF \rangle \\ = \frac{1}{16I(2I-1)} [2(F+I+3)(F-I+2)(I-F+2) \\ \times (F+I-1)(F+I+2)(F-I+1) \\ \times (I-F+1)(F+I)]^{1/2} \eta b_{3/2}. \end{aligned}$$

²² C. Schwartz, Phys. Rev. **97**, 380 (1955).

²³ G. Breit and L. A. Wills, Phys. Rev. **44**, 470 (1933).

The second-order energy is then

$$W_F^{(2)} = (F+I+3)(F-I+2)(I-F+2)(F+I-1) \left\{ \frac{1}{\Delta E_1} \left[\left(\frac{c_1 a_s}{2} - \frac{c_1 a_{3/2}}{2} - \frac{5}{16} \sqrt{2} c_2 \xi a_{3/2} \right) \right. \right. \\ \left. \left. + \frac{I(I+1) - F(F+1) + 3}{4I(2I-1)} (c_1 + \sqrt{2} c_2 \eta) b_{3/2} \right]^2 + \frac{1}{\Delta E_2} \left[\left(\frac{c_1' a_s}{2} - \frac{c_1' a_{3/2}}{2} - \frac{5}{16} \sqrt{2} c_2' \xi a_{3/2} \right) \right. \right. \\ \left. \left. + \frac{I(I+1) - F(F+1) + 3}{4I(2I-1)} (c_1' + \sqrt{2} c_2' \eta) b_{3/2} \right]^2 + \frac{1}{\Delta E_3} \frac{(F+I+2)(F-I+1)(I-F+1)(F+I) b_{3/2}^2 \eta^2}{8I^2(2I-1)^2} \right\}.$$

$\Delta E_{1,2,3}$ are the energy differences between the 3P_2 state and the 3P_1 , 1P_1 , and 3P_0 states, respectively, measured in the same units as the interaction constants. ΔE is positive or negative depending on whether the 3P_2 state lies higher or lower in energy than the other state involved.

The constants necessary for the evaluation of $W_F^{(2)}$ in a specific case are c_1 , c_2 , a_s , $a_{3/2}$, $b_{3/2}$, ξ , and η . For mercury c_1 and c_2 were obtained from the measured g_J value,²⁴ $g_J = 1.4838(4)$, for the 3P_1 state by a method outlined in Breit and Wills.²³ The values of c_1 and c_2 so obtained are $c_1 = 0.4210(20)$ and $c_2 = 0.9071(10)$. With these values of c_1 and c_2 the dipole interaction constant for the 1P_1 state, $A({}^1P_1)$, as calculated from the hyperfine structure measured in the 3P_2 and 3P_1 states agrees quite well with the experimental value. Blaise and Chantrell,²⁵ who obtained c_1 and c_2 by means of the method of Wolfe,²⁶ found a large discrepancy between the value of $A({}^1P_1)$ calculated in this manner and the experimental value. In general it would seem better to use $g_J({}^3P_1)$ to calculate c_1 and c_2 when it is available.

As given by Breit and Wills the dipole interaction constants for the 3P_2 and 3P_1 states are

$$A({}^3P_2) = (1/4)a_s + (3/4)a_{3/2} \\ A({}^3P_1) = (1/4)(2c_2^2 - c_1^2)a_s \\ + [(5/4)c_1^2 - (5\sqrt{2}/16)c_1c_2\xi]a_{3/2} + (1/2)c_2^2a_{1/2}.$$

With the experimental values of $A({}^3P_2)$ and $A({}^3P_1)$ and the theoretical relationship $a_{1/2} = 5\theta(1-\delta)_{1/2}(1-\epsilon)_{1/2}a_{3/2}$ the two equations can be solved simultaneously for a_s and $a_{3/2}$. The notation is generally that of Schwartz²⁷ except for the hyperfine structure anomaly terms δ and ϵ which are given by Kopfermann.²⁸ The values obtained are

$$a_s(199) = 35\,110(80) \text{ Mc/sec,} \\ a_{3/2}(199) = 385(26) \text{ Mc/sec,} \\ a_s(201) = 12\,980(30) \text{ Mc/sec,} \\ a_{3/2}(201) = 142(10) \text{ Mc/sec.}$$

The dipole interaction constants which were used for the 3P_1 state are $A_{199}({}^3P_1) = 491.65$ mK and $A_{201}({}^3P_1) = -181.625$ mK and are an average of the results of Sagalyn *et al.*²⁹ and Blaise and Chantrell.²⁵ The errors quoted for a_s and $a_{3/2}$ are based solely on the estimated errors in c_1 , c_2 , ξ , θ , δ , and ϵ and the stated experimental errors in $A({}^3P_1)$. They do not take into account the possible effects of configuration interaction.

The relativistic correction θ was taken from Schwartz²⁷ and ξ and η were calculated according to Casimir.³⁰ In summary the constants which have not already been given are $b_{3/2} = 399.150$ Mc/sec, $\xi = 1.094$, $\eta = 1.354$, $(1-\delta)_{1/2} = 0.976$, and $(1-\epsilon)_{1/2} = 0.992$.

If the second order energy is calculated with these constants and then subtracted from the measured hyperfine structure intervals the usual first order theory can be used to obtain the corrected interaction constants

$$A_{199}' = 9066.449(3) \text{ Mc/sec,} \\ A_{201}' = -3352.0292(8) \text{ Mc/sec,} \\ B_{201}' = 399.150(2) \text{ Mc/sec,} \\ C_{201}' = -0.00184(9) \text{ Mc/sec.}$$

The ordering of the levels of different F which determines the signs of A_{199}' and A_{201}' was obtained from the optical measurements. The stated uncertainties are due principally to uncertainties in the second order corrections. The uncorrected values for the interaction constants are

$$A_{199} = 9066.6236(20) \text{ Mc/sec,} \\ A_{201} = -3352.00317(19) \text{ Mc/sec,} \\ B_{201} = 399.3180(9) \text{ Mc/sec,} \\ C_{201} = -0.00299(4) \text{ Mc/sec.}$$

The corrections are significant only in the case of C_{201}' . The effect of configuration interaction on the second order corrections has been ignored.

The nuclear octupole moment can be obtained from the relation $\Omega = (7cgIF_{3/2}/a_{3/2}TZ^2)a_0^3 \times 10^{24}$ nmb [where 1 nmb \equiv 1 nuclear magneton barn $= (e\hbar/2Mc) \times 10^{-24}$ cm²]. The value so obtained is $\Omega = -0.130(13)$ nmb,

²⁴ J. Brossel and F. Bitter, *Phys. Rev.* **86**, 308 (1952).

²⁵ J. Blaise and H. Chantrell, *J. phys. radium* **18**, 193 (1957).

²⁶ H. C. Wolfe, *Phys. Rev.* **41**, 443 (1932).

²⁷ C. Schwartz, *Phys. Rev.* **105**, 173 (1957).

²⁸ H. Kopfermann, *Nuclear Moments* (Academic Press, Inc., New York, 1958), 2nd ed., pp. 129-130.

²⁹ P. L. Sagalyn, A. C. Melissinos, and F. Bitter, *Phys. Rev.* **109**, 375 (1958).

³⁰ H. B. G. Casimir, *On the Interaction between Atomic Nuclei and Electrons* (Teyler's Tweede Genootschap, Haarlem, 1936).

where $T/F_{3/2}=1.14$ has been obtained from Schwartz.²⁷ In deriving the value of C' the correction due to configuration mixing has been ignored. The extreme single particle model gives for a single $p_{3/2}$ neutron $\Omega=-0.34$ nmb. Hg^{201} is the first odd neutron nucleus for which an octupole moment has been measured. The moment bears about the same relation to the single particle value as has been noted for the octupole moments of odd proton nuclei. It would be interesting to see if the independent particle model including configuration mixing, which is fairly successful in predicting the dipole moment of Hg^{201} , could also correctly predict the octupole moment.

The quadrupole moment obtained from B_{201}' is $Q=[(8/3)b_{3/2}g_I F_{3/2}/a_{3/2}R](\mu_0^2/e^2)(m/M_p)\times 10^{24}$ barns = 0.50(4) barns, where $F_{3/2}/R=0.889$. This value is to be compared with $Q=0.46$ barns obtained by Murakawa¹⁶ who has taken into account the effects of an admixture of $(5d^96s^26p)^3P_2$ state. Sternheimer³¹ type polarization corrections are not included in the above values of Q although Murakawa has made an estimate of such corrections and obtains $Q=0.42$ barn. The same corrections applied to the value for Q obtained in the present work give $Q=0.45_5(4)$ barn.

The mercury isotopes are the first case of odd-neutron, even-proton nuclei for which a hyperfine structure anomaly has been measured. The quantity which can be compared with theoretical predictions is the anomaly for the s electrons alone, $\Delta(s_{1/2})$. A simple calculation gives

$$\Delta(s_{1/2}) = \left[\frac{A_{199} g_I(201)}{A_{201} g_I(199)} - 1 \right] \left[1 + 3 \frac{a_{3/2}(201)}{a_s(201)} \right].$$

With the value $g_{199}/g_{201} = -2.70902(3)$ given by Cagnac and Brossel³² the anomaly is $\Delta(s_{1/2}) = -0.1728(12)\%$.

³¹ R. M. Sternheimer, Phys. Rev. **95**, 736 (1954); **105**, 158 (1957).

³² B. Cagnac and J. Brossel, Compt. rend. **249**, 77 (1959).

A measurement³³ of the Knight shift in metallic mercury gives $\Delta(s_{1/2}) = -0.16(10)\%$. The anomaly, $\Delta(s_{1/2})$, calculated on the extreme single particle model as outlined by Eisinger and Jaccarino³⁴ and Stroke³⁵ is -1.1% . Although the single particle model predicts the moment of Hg^{199} fairly well it gives an answer for the moment of Hg^{201} which differs considerably from the experimentally determined value and in addition fails to predict a non-zero quadrupole moment. At present there are no calculations of the anomaly based on other models, such as the independent particle model with configuration mixing, with which to compare the experimental results.

ACKNOWLEDGMENTS

The authors wish to thank W. L. Faust and Dr. L. C. McDermott for aid in taking and reducing the data, also for the valuable aid of Dr. McDermott in checking the computations. They also thank the Watson Scientific Computing Laboratory of IBM for time generously donated on the 650 computer. Many thanks are due to Dr. K. King for programming and carrying out the computations involved in extracting the eigenvalues of the energy matrix for Hg^{201} .

Grateful recognition is extended to Professor K. Murakawa for his kind permission to quote his results on the states of mercury prior to publication. Professor D. G. Ravenhall and Professor R. Novick of the University of Illinois are to be thanked for helpful discussions concerning some of the theoretical problems treated in the paper.

Finally, the authors wish especially to thank Professor P. Kusch for many helpful suggestions as well as interest and encouragement in the experiment.

³³ J. Eisinger, W. E. Blumberg, and R. E. Shulman, Bull. Am. Phys. Soc. **4**, 451 (1959).

³⁴ J. Eisinger and V. Jaccarino, Revs. Modern Phys. **30**, 528 (1958).

³⁵ H. H. Stroke, Quarterly Progress Report, Research Laboratory of Electronics, Massachusetts Institute of Technology, July 15, 1959 (unpublished), p. 63.